Verification of Complex Excitation Coefficients from Measured Space Array Antenna by the Equivalent Current Technique

L. Salghetti Drioli
European Space Agency, ESA/ESTEC,
2200AG Noordwijk, The Netherlands,
Luca.Salghetti.Drioli@esa.int

L.J. Foged, F. Saccardi, L. Scialacqua
Microwave Vision Italy, MVI,
Via dei Castelli Romani 59, Pomezia, Italy
lars.foged@microwavevision.com

***Abstract*— In this paper the inverse-source technique or source reconstruction technique has been applied as diagnostic tool to determine the complex excitation at sub array and single element level of a measured array antenna [1]-[5]. The inverse-source technique, implemented in the commercially available tool "INSIGHT" [5], allows to compute equivalent electric and magnetic currents providing exclusive diagnostic information about the measured antenna. By additional processing of the equivalent currents the user can gain insight to the realized excitation law at single element and sub-array level to identify possible errors.**

The array investigated in this paper is intended as part of the European Navigation System GALILEO and is a pre-development model flying on the In-Orbit Validation Element the GIOVE-B satellite. The antenna, developed by EADS-CASA Espacio, consists of 42 patch elements, divided into six sectors and is fed by a two level beam forming network (BFN). The BFN provide complex excitation coefficients of each array element to obtain the desired iso-flux shaped beam pattern [6]-[7]. The measurements have been performed in the new hybrid (Near Field and Compact Range) facility in the ESTEC CPTR as part of the installation and validation procedure [8]. The investigation has been performed without any prior information of the array and intended excitation. The input data for the analysis is the measured spherical NF data and the array topology and reference coordinate system.

I. INTRODUCTION

The inverse-source technique or equivalent current approach (EQC) provides advanced antenna measurement post-processing. The technique [1]-[3] is implemented in the commercially available code "MV-INSIGHT" [5]. Based on the acquired Near Field (NF) or Far Field (FF) data, the equivalent electric and magnetic radiating currents can be determined on an arbitrary shaped reconstruction surface conformal to the test object. The availability of the equivalent currents is a key point for the analysis/post-processing of measured antennas since they can be used for diagnostic purposes and also to improve the measurement accuracy [3].

In this paper, MV-INSIGHT has been used in the diagnostic analysis of the GIOVE-B array antenna. The antenna has been measured in the new Spherical Near Field System (SNF) located in the ESA Compact Payload Test Range (CPTR). The antenna consist of 42 stacked patches on a regular grid within a 1.3 m diameter envelope, corresponding to 5.2λ @ 1192 MHz. The antenna has an iso-flux pattern, covering an angular domain of +/- 13 deg, corresponding to the Earth view angle from a Medium Earth Orbit (MEO). The antenna is right hand circularly polarized [6].

The array antenna during measurement in the SNF system in the ESA CPTR is shown in Fig. 1. The measured co-polar and cx-polar radiation pattern @ 1192 MHz is illustrated in the top part of Fig. 2 for the horizontal (ϕ = 0°), vertical (ϕ = 90°) and diagonals (ϕ = 45°, ϕ = 135°) cuts. A zoom of the main-beam co-polar pattern is shown in the bottom part of Fig. 2.

Figure 1. The GIOVE-B array antenna during measurements in the new near field upgrade of the ESTEC CPTR system.

The measured pattern of the GIOVE-B array antenna shows deviations with respect to predicted/attended results. The axial pattern symmetry and the End-Of-Coverage (EOC) gain, is in fact not as good as expected. On the other hand, the measurement confirm very low cross polar levels in the bore-sight direction.

The root causes of the axial pattern asymmetry as well as the design mechanism behind the achieved on-axis cross polar performance will be investigated in this paper using MV-INSIGHT as diagnostic tool. Furthermore, a filtering technique [3] available in MV-INSIGHT, will be exploited to isolate the sub-array elements of the antenna and thus verify the realized complex excitation coefficients.

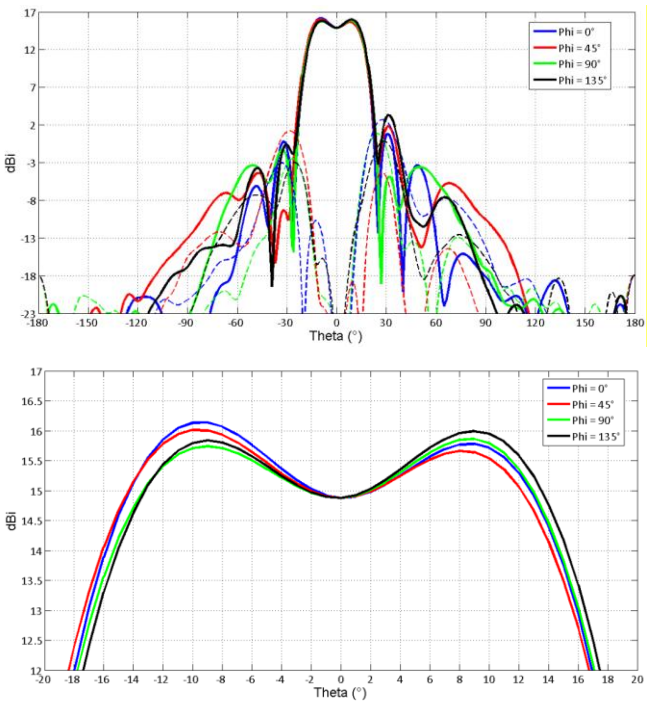

Figure 2. Radiation pattern @ 1192MHz of the GIOVE-B array antenna measured in the Spherical NF system at ESTEC CPTR (top). Zoom on the main beam of the co-polar radiation pattern (Bottom).

II. Equivalent Currents Model of the Array

The EQC technique has been applied to the measurement of the GIOVE-B antenna considering a cylinder with a diameter of 1.6m and a height of 0.6m fully enclosing the antenna as equivalent surface. Furthermore, in order to diagnose possibly interactions with the supporting structure of the antenna, an additional cylinder fully enclosing the stand-off used for the near field measurement has been also considered in the equivalent surface. The equivalent electric currents on 3D structure computed by the EQC technique are reported in Fig. 3.

From a first analysis of the top part of the equivalent structure (aperture of the array), an hexagonal central section excited with higher amplitude weighting coefficients, can be clearly identified. Moreover a secondary section of elements excited with minor amplitude coefficients is detected on the annular circular section. This distribution is in agreement with the expected distribution coming from the amplitude and phase weighting of the array elements and needed to shape the beam to an iso-flux pattern. In order to better understand the radiation mechanism and find out possible root causes of the anomalies observed in the measured radiation pattern of the of the GIOVE-B array, the currents lying on the aperture of the antenna will be analyzed with more detail in the next sections.

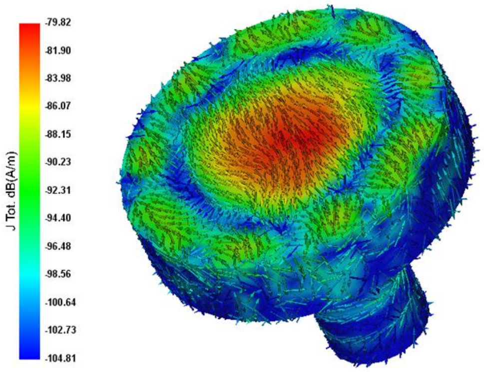

Figure 3. Equivalent currents on the whole antenna structure plus the Stand-off used to perform the NF measurement.

III. Analysis of Axial Symmetry

In order to investigate the root causes of the axis asymmetry observed in the measured radiation pattern of the GIOVE-B shown in Fig. 2, the co-polarized (RHCP) equivalent currents computed by the EQC method are analysed in this section.

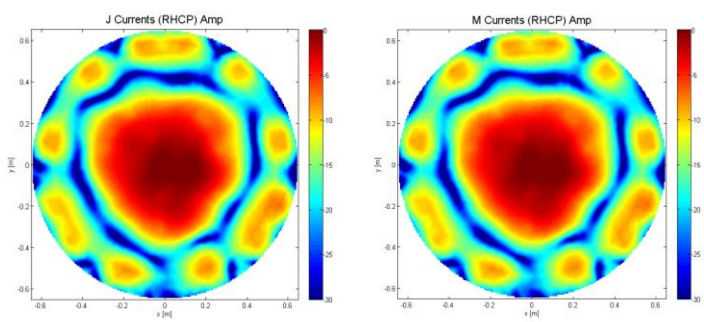

Figure 4. Amplitude of the Co-polarized electric (left) and magnetic (right) currents of the GIOVE-B array determined by the EQC technique.

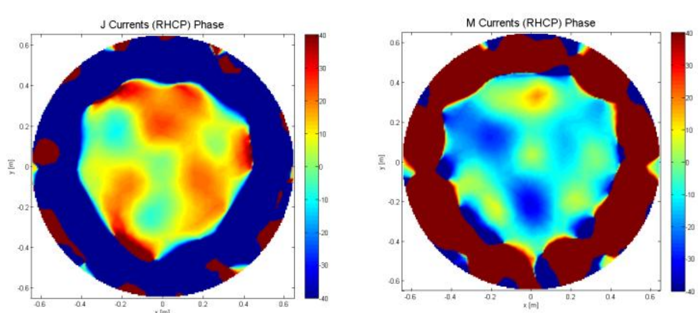

Figure 5. Phase of the Co-polarized electric (left) and magnetic (right) currents of the GIOVE-B array determined by the EQC technique.

The normalized amplitude (wrt the peak of the co-polar distribution) of the co-polarized electric and magnetic currents are reported in Fig. 4. As can be seen from the amplitude of the co-polarized currents, a nice symmetric excitation is obtained in the central elements of the array.

The co-polar electric and magnetic current phase distributions are reported in Fig. 5 on a normalized +/- 40° scale. Some phase dispersion on the central elements can be noted on both distributions. In particular, approximately up to 30° phase deviation is observed in the central part of the array. Such phase dispersion is one of the contributing factors to the axial asymmetry observed in the measured radiation pattern of the GIOVE-B array.

IV. Analysis of the On-Axis Cx-Polar Performance

In order to discover the design mechanism behind the achieved on-axis cross polar performance observed in the measured radiation pattern shown in Fig. 2, the cx-polarized (LHCP) equivalent currents computed by the EQC method are analyzed in this section.

The normalized amplitude of the cx-polarized electric and magnetic currents are reported in Fig. 6. The levels have been normalized wrt the peak of the co-polar distribution. Similarly, the corresponding phase distributions of the cx-polarized electric and magnetic currents are reported in Fig. 7 on a +/- 180° scale.

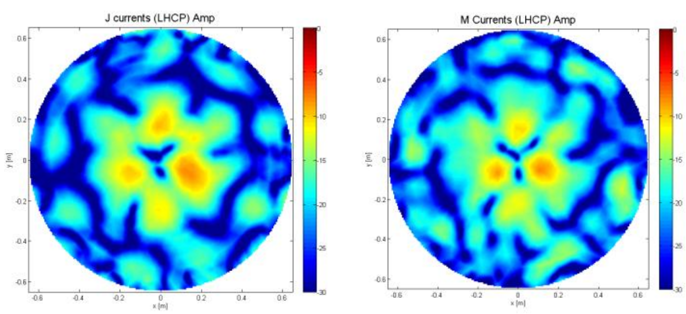

Figure 6. Amplitude of the Cx-polarized electric (left) and magnetic (right) currents of the GIOVE-B array determined by the EQC technique.

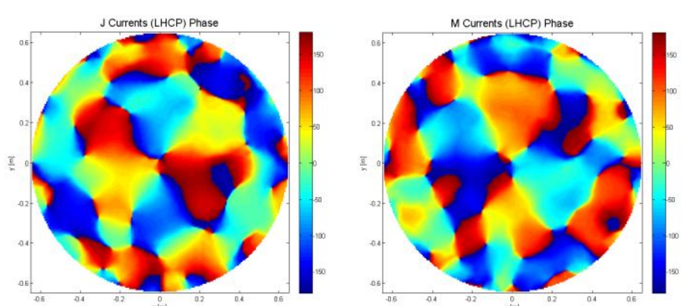

Figure 7. Phase of the Cx-polarized electric (left) and magnetic (right) currents of the GIOVE-B array determined by the EQC technique.

As can be seen from the amplitude of the currents associated to the central part of the array, the cx-polar excitation is surprisingly high at single element level, only approximately 12 dB below the co-polar peak. Nevertheless, the on-axis cx-polar radiation of the entire array is very low, as desired from a well-designed antenna as observed previously. The reason for this phenomena is clearly visible by the cx-polar phase distribution shown in Fig. 7. The on-axis performance have in fact been optimized by sequential rotation of the array elements. The phase distribution shown that a three-elements sequential rotation scheme has been adopted. Consequently, three different phase shifts have been implemented in the BFN (-120°, 0°, +120°) in order to shape the cross polar pattern, creating a null in the boresight direction while maintaining the in-phase co-polar excitation. It should be noted, that such a complex feeding mechanism for the optimization of the array cx-polar performance could give rise to some residual phase errors regarding the co-polar performance. Obtaining an accurate +/-120° phase shift is rather demanding especially over a relative large bandwidth. This could most probably explain the root cause of the observed co-polar phase dispersion discovered in the previous section and shown in Fig. 5. Thus, the nice cross-polar performance of the array carries a price in terms of achieved co-polar axial asymmetry of the radiation pattern.

V. Analysis of Complex Exitation with Spatial Filtering of Equivalent Currents

In this section the complex excitation at sub-array level has been verified exploiting the spatial filtering functionalities available in MV-INSIGHT.

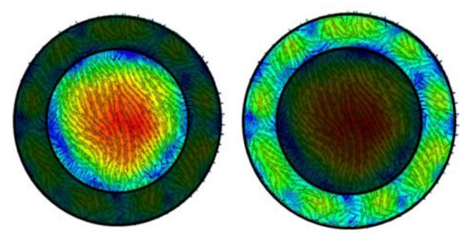

Figure 8. Equivalent currents associated to the inner ring (Left) and associated to the outer ring (Right).

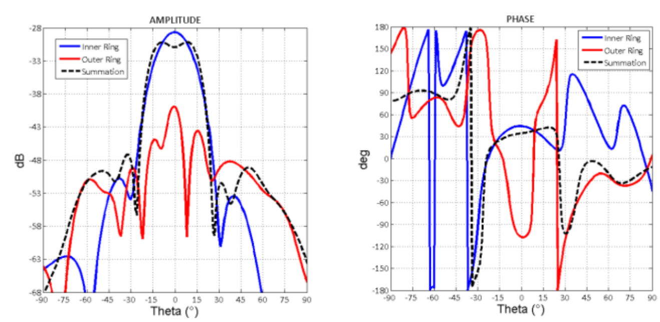

Figure 9. Separation of different contributions to the co-polar radiation pattern along vertical cut: inner ring pattern (Blue), outer ring pattern (Red).

First of all, the equivalent currents associated to the central section of the array (inner ring) have been isolated from the lateral section (outer ring) in order to evaluate their contribute to the radiation. To do that, the two filtering-masks shown in Fig. 8 have been used in order evaluate the two separate contributions needed to create the wanted iso-flux pattern. The co-polar radiation pattern contributions associated respectively to the inner and outer ring currents are shown in Fig. 9 for both amplitude and phase. As can be seen, both contributes are not symmetric as expected. In particular, the asymmetry of the outer ring is well highlighted thanks to the isolation of the corresponding currents. The reason of such asymmetry is most probably due to a problem in the BFN.

Subsequently, the spatial filtering functionality of MV-INSIGHT have also been used to isolate three sub-array sections located on the outer annular ring from the hexagonal central section. The four different set of equivalent currents obtained after spatial filtering of the full set of currents are illustrated in the first column of Table I.

TABLE I. VERIFICATION OF SUB-ARRAY COMPLEX EXCITATION

Current Isolation	**Radition Pattern**	**Complex Excitation**
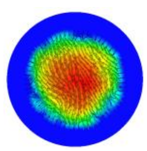	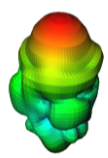	Amp: 0.00 dB Phase: 0.00°
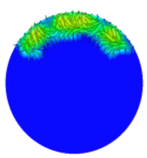	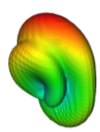	Amp: -18.76 dB Phase: -184.06°
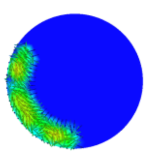	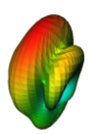	Amp: -18.45 dB Phase: -166.89°
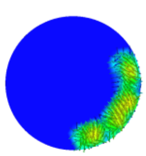	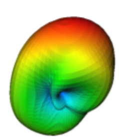	Amp: -17.85 dB Phase: -161.52°

This sub-array parts are not real building block of the antenna which is in fact composed of three sectors, each of them includes both elements from the centre area and outer ring [8].

The four radiation pattern associated to the corresponding four set of spatial filtered equivalent currents are shown in the second column of Table I. The complex excitation coefficients of the four sub-array sections have been obtained computing for each section the total radiated power over the full sphere and taking the phase value on the boresight direction. The obtained complex coefficients normalized wrt the central sub-array section are reported in the third column of Table I.

The determined complex values are reasonably in line with the expected values especially regarding the amplitude. The obtained excitation phase is also quite good. In fact the wanted phase shift of 0°/180° between central elements and outer elements have been reached with-in less than 20° error in the worst case. This excitation error also contribute to the co-polar axial asymmetry of the radiation pattern as shown Fig. 2.

VI. CONCLUSION

The potentialities of the inverse source technique implemented within the MV-INSIGHT software have been exploited in this paper in order to analyze the GIOVE-B array antenna. The antenna has been measured in the new ESA CPTR/NF hybrid system. The measured radiation pattern showed some deviations with respect to predicted/attended results especially regarding the axial symmetry and the End-Of-Coverage (EOC) gain. On the other hand the array design confirmed a remarkably low cross polar levels in the bore-sight direction. The root causes of the axial asymmetry as well as the design mechanism behind the achieved on-axis cross polar performance has thus been investigated in this paper using MV-INSIGHT as diagnostic tool. The analysis performed on the cx-polarized equivalent currents determined by MV-INSIGHT, clearly illustrate the applied three-elements sequential rotation strategy behind the very nice cross-polar performance of the GIOVE-B array. This mechanism has been discovered without accessing any a-priori array design information. The equivalent current analysis also allowed to discover the co-polar phase dispersion as a possible root cause or contribution to the axial asymmetry of the pattern. Furthermore, a filtering technique available in the software, has been exploited to isolate the sub-array elements on the outer annular ring of the array to verify the realized complex excitation coefficients. The amplitude and phase dispersion of these element excitation also contribute to the axial asymmetry of the pattern.

REFERENCES

[1] J. L. Araque Quijano, G. Vecchi. Improved accuracy source reconstruction on arbitrary 3-D surfaces. Antennas and Wireless Propagation Letters, IEEE, 8:1046–1049, 2009.

[2] L. Scialacqua, F. Saccardi, L. J. Foged, J. L. Araque Quijano, G. Vecchi, M. Sabbadini, “Practical Application of the Equivalent Source Method as an Antenna Diagnostics Tool”, AMTA Symposium, October 2011, Englewood, Colorado, USA

[3] J. L. Araque Quijano, L. Scialacqua, J. Zackrisson, L. J. Foged, M. Sabbadini, G. Vecchi “Suppression of undesired radiated fields based on equivalent currents reconstruction from measured data”, IEEE Antenna and wireless propagation letters, vol. 10, 2011 p314-317.

[4] L. J. Foged, L. Scialacqua, F. Mioc,F. Saccardi, P. O. Iversen, L. Shmidov, R. Braun, J. L. Araque Quijano, G. Vecchi " Echo Suppresion by Spatial Filtering Techniques in Advanced Planar and Spherical NF Antenna Measurements ", AMTA Symposium, October 2012, Seattle, Washington, USA

[5] http://www.satimo.com/software/insight

[6] A. Montesano, F. Monjas, L.E. Cuesta, A. Olea, “GALILEO System Navigation Antenna for Global Positioning”, 28th ESA Antenna Workshop on Space

[7] L.S. Drioli, C. Mangenot, “Microwave holography as a diagnostic tools: an application to the galileo navigation antenna”, 30th Annual Antenna Measurement Techniques Association Symposium, AMTA 2008, Boston, Massachusetts November 2008

[8] S. Burgos, M. Boumans, P. O. Iversen, C. Veiglhuber, U. Wagner, P. Miller, “Hybrid test range in the ESTEC compact payload test range”, 35th ESA Antenna Workshop on Antenna and Free Space RF Measurements ESA/ESTEC, The Netherlands, September 201